Third Joint Eurohaptics Conference and Symposium on Haptic Interfaces
for Virtual Environment and Teleoperator Systems
Salt Lake City, UT, USA, March 18-20, 2009

Variable Resistance Hand Device Using an Electro-Rheological Fluid Damper

B. Weinberg[1], A. Khanicheh[1], M. Sivak[1], O. Unluhisarcikli[1], G. Morel[2],
J. Shannon[3], J. Kelliher[3], M. Sabadosa[3], G. Bonmassar[4], B. Patritti[5], P. Bonato[5] and C. Mavroidis[1,*]

[1]Department of Mechanical and Industrial Engineering, Northeastern University, Boston, MA, USA
[2]Institut Systemes Intelligents et Robotique, University Paris VI, Paris, France
[3]WGI, Inc., 34 Hudson Drive, Southwick MA, USA
[4]Martinos Center for Biomedical Imaging, Massachusetts General Hospital, Boston, MA, USA
[5]Spaulding Rehabilitation Hospital, Boston, MA, USA

*Corresponding Author: mavro@coe.neu.edu ; 617-373-4121; http://www.coe.neu.edu/~mavro

ABSTRACT

This paper presents the design, fabrication, control and testing of the third generation prototype of a novel, one degree of freedom (DOF) Variable Resistance Hand Device (VRHD) that was designed for isotonic, isokinetic, and variable resistance grasp and release exercises. Its principle functionality is derived from an electro-rheological fluid based controllable damper that allows continuously variable modulation of dynamic resistance throughout its stroke. The VRHD system consists of the patient actuated device, the control electronics and software, the practitioner graphical interface and the patient's virtual reality game software. VRHD was designed and experimentally shown to be fully Magnetic Resonance Imaging (MRI) compatible so that it can be used in brain MR imaging during handgrip rehabilitation.

1 INTRODUCTION

Of all impairments that result from stroke, perhaps the most disabling is hemiparesis of the upper limb because the impact on disability, independence and quality of life is so marked [1]. Stroke survivors typically receive intensive, hands-on physical and occupational therapy to encourage motor recovery. However, due to economic pressures on national care systems, individuals post stroke are receiving less therapy and are discharged from rehabilitation hospitals sooner than it used to be. Robotic / force feedback training is a considerably new technology that shows great potential for application in the field of neurorehabilitation as it has several advantages e.g., motivation, adaptability, data collection, and the ability to provide intensive individualized repetitive practice [2]. Studies on robotic / force feedback devices for upper extremity rehabilitation after stroke have shown significant increases in upper limb function, dexterity and fine motor manipulations [3] as well as improved proximal motor control [4].

Furthermore, functional MRI (fMRI) has been widely used in studying human brain mechanisms controlling voluntary movement and reorganization of the sensorimotor brain system in response to neurological injuries such as stroke [5]. A force feedback system is capable of controlling and quantifying changes in movement kinematics and kinetics. Therefore, it enables clinicians who perform fMRI to quantify and monitor the effect of motor retraining in neurological patients such as stroke, and improve the practice of neurorehabilitation. fMRI compatible force feedback devices, such as the one presented in this paper, will allow one to conduct with the same device evaluation and training of motor performance, as well as evaluation of movement-related brain activity underlying the response of stroke patients to motor retraining. Due to high magnetic fields, fast-switching magnetic field gradients and radiofrequency pulses in MRI, the development of any mechatronic system that could be used inside this modality is challenging. Despite these challenges, force feedback interfaces which enable neurologists to investigate motor performance and the mechanisms of neural recovery following neurological injuries have been developed [6-12].

In an effort to develop force-feedback devices that can be used in fMRI studies, during the last 3 years, our team has developed novel, compact force feedback devices to facilitate retraining of hand grasp / release in patients recovering from neurological ailments such as stroke [13-15]. The aim is that these systems could be used as evaluation tools to implement innovative rehabilitation protocols in the clinical setting. A key feature of the devices is the use of electro rheological fluids (ERF) to achieve tunable, computer controlled, resistive force generation. For this purpose, the change in yield stress observed in ERFs in response to an electric field was exploited to produce virtually zero resistance when idle and high resistivity when an electric field is applied to the ERF. Our devices are fMRI compatible so as to allow one to evaluate patients for changes in brain activity associated with motor retraining.

Our first prototype, shown in Fig. 1-TOP, incorporated a pincer handle motion with a rotary ERF brake [13]. While the device was shown to be MR compatible and had adequate performance as a rehabilitation tool, it had limitations related to friction, weight and eddy current effects. Our experience with the first prototype and an increased understanding of the MR environment led to the design and fabrication of a second, completely different prototype. The VRHD V2, shown in Fig. 1-MIDDLE, incorporated a linear handle motion with a linear ERF damper. This prototype was stronger and had lower friction than the V1 prototype [14, 15]. The compatibility of VRHD V2 inside MRI environment was tested successfully through comprehensive phantom and human experiments. (Fig.1-BOTTOM).

In this paper, we present the third generation (V3) prototype of VRHD. Several important improvements have been made and new features added that include: a) deriving the design criteria of the system by measures from subjects post-stroke. Specifically, we were interested in determining the maximum amount of friction that could be tolerated when using the system in pa-

tients post-stroke; b) a new damper design that reduces significantly friction and increases maximum force output; c) a dynamometer feature that allows the device to be operated as a static grip force measuring device by locking the shaft; d) a new closed loop controller with the addition of a new graphic user interface for the medical practitioner that allows accurate and smooth operation of the device combined with increased patient's motivation level.

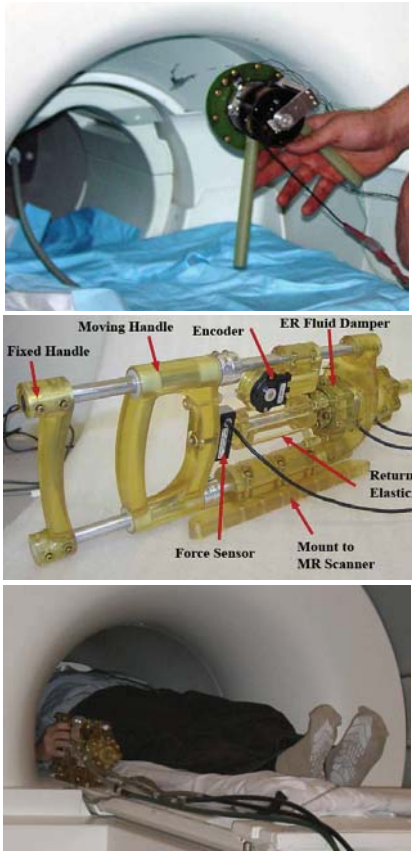

Figure 1. Variable Resistance Hand Device (VRHD) V1 with rotary ERF brake (TOP); VRHD V2 with linear ERF damper (MIDDLE); VRHD V2 being used inside the scanner during fMRI testing (BOTTOM).

2 Grasp and Release Tests in Patients Post-stroke

Grip strength is usually measured using a hand dynamometer which performs isometric measurements. It was observed that the maximum force of squeezing a dynamometer with fixed handles (isometric measurements of the hand grip) is different than the maximum force of squeezing the VRHD with moving handles (isotonic or isokinetic measurements of the hand grip). To our knowledge, no data in the literature is available on the dynamic hand grip strength post stroke. Therefore, a study was performed to evaluate the grip strength of individual post stroke performing repetitive grasp and release movements to define the acceptance range of resistive forces applied by VRHD to the hand.

A total of 19 community dwelling adults (> 35 years old) in the chronic stages of recovery from a single stroke (≥1 year post insult) with upper extremity paresis were enrolled in the study. Subjects displayed some upper extremity impairments but were able to flex and extend their impaired hand's metacarpal–phalangeal joints (MCPJ) at least 25% of the range (~20 degrees).

Tests were completed with a spring-tensioned linear device similar in design to the VRHD, which has a similar interface (i.e. handle) with the subject. However, it relied on a spring to simulate the friction associated with the ERF components. The tests with the spring device were planned to derive design characteristics regarding the maximum amount of friction that can be tolerated by patients post-stroke in performing dynamic grasp and release movements with their impaired hand.

We assessed the ability of individuals post-stroke to perform repetitive grasp and release movements (5 repetitions) at their comfortable speed in both seated and supine positions. The seated tests preceded the supine tests. Subjects were positioned in each posture (seated and supine) so they could comfortably grasp the handle of the device. Adjustments in (1) the position and orientation of the device with respect to the body of the subject, and (2) tilt of the device were made on an individual basis so as to maximize the ability of the subject to perform the necessary grasp and release movements. All subjects participated in the testing procedures outlined below.

Subjects were instructed to grasp the handle of the device to establish a baseline position (i.e. stroke length/ROM). The initial spring tension was set on the basis of the mean grip force measured using the grip dynamometer. For mean grip forces ≤ 60 N the starting spring tension was set to 50 % of the mean grip force value. For mean grip forces ≥ 60 N the starting spring tension was set to 30 N, the maximum tension possible with the springs used.

A total of 16 of the 19 subjects displayed a functional ability with their hand that allowed them to use the device. The remaining 3 subjects did not have adequate grasp and release function to be able to assess grip strength adequately or use the device. The results of the 16 subjects who completed the grip strength are summarized in **Table 1**. Mean grip strength assessed with the dynamometer was greater in the seated position compared to the supine position. The mean stroke length was the same in the seated and supine position. Subjects generally performed the 5 RM (repletion maximum) tests at a slightly faster comfortable speed in the seated position compared to the supine position, as measured by the time to complete the 5 RMs. For the tests of 5 RM, 13/16 subjects in the seated position and 10/16 in the supine position achieved the maximum possible 5 RM of 30 N (i.e. maximum possible spring tension). The mean 5 RM in the seated position was greater than that recorded for the supine position.

Table 1, Grip strength for the 16 subjects who were able to perform the 5 RM grasp and release movements.

	Seated Tests		Supine Tests	
	Mean ± SD	Range (min-max)	Mean ± SD	Range (min-max)
Grip strength (N)	123.4 ± 94.5	19.6 – 398.9	93.7 ± 88.5	9.8 – 349.9
Stroke length (mm)	24.3 ± 10.4	9 – 41	24.3 ± 10.4	9 – 41
Timed 5RM (s)	11.4 ± 7.8	5.3 – 34.9	12.9s ± 10.3	3.6 – 40.6
Successful 5RM (N)	27.8 ± 4.6	18.5 – 30	22.4 ± 9.6	9.5 – 30

3 Design and Prototype Development

The VRHD V3 (Fig. 2) consists of the handles, sensors, controllable damper, handle return system, dynometer lock, and the

support structure. The design specifications of the VRHD, that were fully met in the final prototype, are shown in **Table 2**. These were based on the experimental data obtained in Section 2 and shown in Table 1.

Table 2. VRHD Specifications

Damper Zero Field Resistive Force	2.5N @ 5 cm/sec piston speed
Maximum Resistive Force	200N
Range of Return Force Adjustment	10N - 60N
Stroke Length	5 cm
Weight of Device	2 kg
Overall Length	45 cm

To use the device, a person would grasp the handle and squeeze. The damper will modulate the resistance to a preset level throughout the stroke. After the stroke is complete the damper is deactivated and the handle return system brings the handle back to its resting open position. A pair, one on each side of the moving handle, of adjustable shaft collars determines the starting and ending position of the stroke. The location of these collars can be set using a removable scale (ruler).

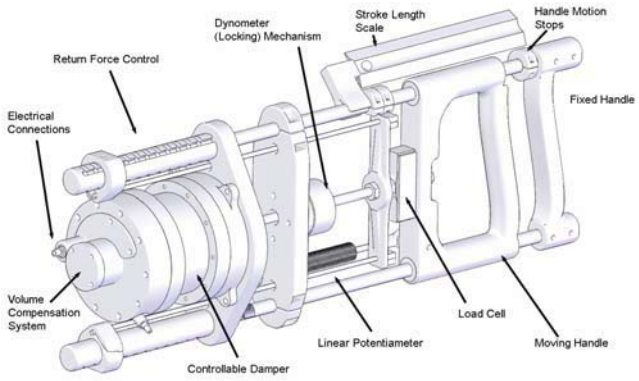

Figure 2. 3D solid model of VRHD and its components

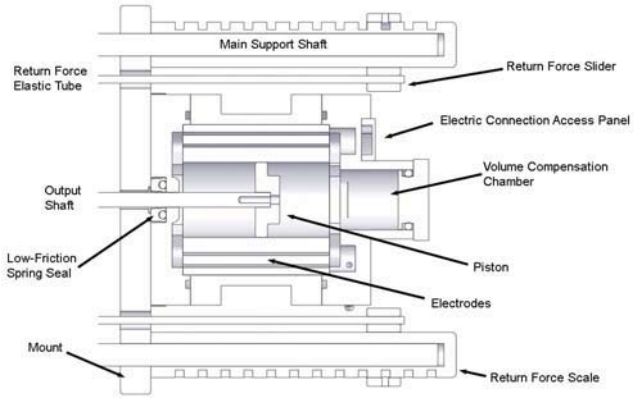

Figure 3. The ERF controllable damper

The controllable damper, shown in Fig. 3, is the main component of the device. This is an ERF based continuously variable computer controlled damping system that provides smooth resistance throughout its range. The controllable damper for VRHD is a new design that offers significant performance advantages over previous versions including reduced no field resistance, increased force capabilities, and reduced size. The handles actuate the internal piston which then forces fluid through the concentric gaps of the ERF valve as the piston moves. ERF responds to electric fields by thickening and when the electric field across the gaps is modulated by the software, a controllable pressure drop across the valve (Fig. 3) is obtained. This pressure is felt by the user squeezing the handles as a resistive force. ERF has a response time on the order of milliseconds so accurate force control is possible.

Several improvements were made to reduce seal friction and the flow restriction through the ERF valve. Precision machining was utilized throughout. A piston seal (a significant friction source) was excluded, replaced instead by a tight piston-bore radial clearance of .0025" to control leakage past the piston. To minimize friction on the output shaft, a custom spring seal was used and all sliding surfaces were coated with a low friction anodized coating. The number of concentric gaps in the ERF valve was increased from one to two to decrease the flow restriction of the ERF fluid when in its inactivated state.

To accommodate changes in volume, a chamber filled with closed cell foam was incorporated into the design. This method of volume compensation was very effective and reduces the complexity of the device. A Buna / Neopreme based closed cell foam was used due to its compatibility with oils, its low spring rate and good compression recovery.

To control the handle return speed or grip release force, an elastic based return system was implemented. A pair of surgical silicone tubes are attached to a bracket mounted next to the load cell (Fig. 2). The other ends are attached to a set of sliding fixtures that control the preload of each silicone tube (Fig. 3). The slider mates with a notched scale that slides over the main support shafts. By adjusting the position of the sliders the preload on the bands can be adjusted.

The Dynometer Locking Mechanism can lock the output shaft in position when needed. This changes the functionality of the device from a dynamic force controlled device to a static measuring device that can measure grip strength with the handles in any position. A clip on ruler is used to reference the position of the handle motion stops which allow the practitioner to adjust the stroke start and end to accommodate varying patient needs.

To provide positional feedback to the software controller, a custom linear potentiometer by Active Sensors UK is implemented. For force measurement, a 150lb (~667N) load cell by Interface Force, USA is mounted to the moving handle. This directly measures the force as applied by the user. The moving handle rides on low friction Igus plain bushings and is shaped ergonomically (in conjunction with the fixed handle) to provide maximum user comfort. The VRHD V3 is shown in Fig. 4.

Figure 4. The Variable Resistance Hand Device V3 and its Graphical User Interface.

4 Closed Loop Control

A typical grasp and release exercise consists of either an isokinetic (constant speed) or an isotonic (constant force) motion. In this section we present our closed loop controller designed to implement isotonic (constant force) exercise schemes in an ac-

curate and smooth way. A major challenge in implementing a force control algorithm in an ERF controlled device such as the VRHD, is that it can only resist and does not produce any "active" force. In fact, it has to act as a brake in order to input a disturbance in the human motor loop so as to finally exhibit a constant force. In other words, the human being must be able of applying the force. For example, suppose that during the isotonic exercise, we want the force to be equal to a given value F_d. Initially, the device is still. While the force is lower than F_d, the device should stay still. When the device starts moving, it seems natural that the force applied by the operator decreases. Reacting too fast to this decrease in order to increase the force, it maybe unnatural and may lead to stopping the device. In other words, it is natural to leave a little bit of *Stribeck* effect.

The block diagram of the implemented controller for isotonic exercises is shown in Fig. 5. In this control scheme, F_d (in red) is the value that is set in the interface by the practitioner, with the interface unit entered (see Fig. 7). Zeros are respected, meaning that if all the inputs are zero (in natural units) then the output voltage (really applied to the device) is zero Volts. The feed-forward term, and eventually the gains, can be computed as nonlinear functions of the position, the velocity and the desired force. Also, integral control with anti-windup has been investigated for the force loop.

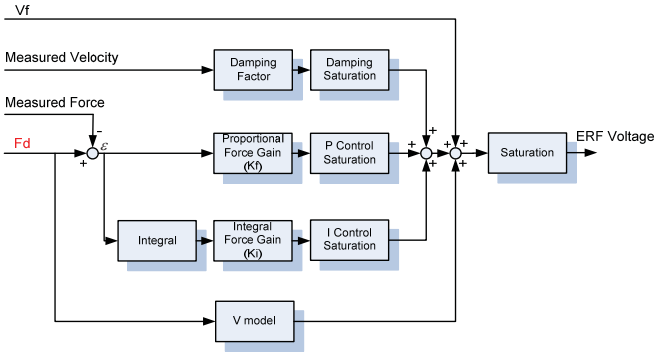

Figure 5. Block diagram of the controller for isotonic exercises.

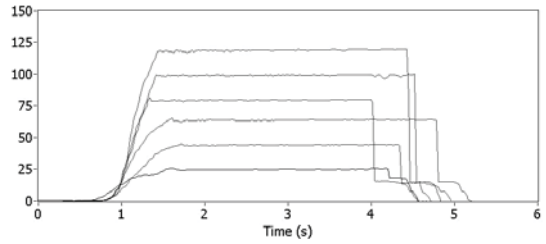

Figure 6. Constant force experiment under PI for 25, 45, 65, 80, 100, 120 (N).

The proportional term makes a change to the output that is proportional to the force error value. The proportional response is adjusted by multiplying the error by a constant K_f. The saturation term is the high and low limit of the output voltage sent to the ERF. The integral term (when added to the proportional term) accelerates the movement of the process towards setpoint and eliminates the residual steady-state error that occurs with a proportional only controller. The magnitude of the contribution of the integral term to the overall control action is determined by the integral gain, K_i. The integral anti-windup is making sure that the integral is kept to a proper value and avoids the output voltage saturation. The feedforward term V_{model} was obtained experimentally from open loop testing:

$$V_{model}=0.027*F_d+0.29$$

The V_{model} generates the output voltage to the ERF linearly as a function of the input desired force F_d. A damping factor could also be used in the control of the system to take into account the velocity dependence of the force generated by the system. To improve the performance of the PI Controller gain scheduling was used, meaning individual gains were calculated for different intervals of force. The graph in Fig. 6 shows several example results for closed loop force control experiments where the desired force is set at 25, 45, 65, 80, 100, 120 (N).

For the implementation of the controller, the LabVIEW graphical programming language running on a Real-Time Operating System (RTOS) has been used. Since the system runs on a RTOS, the code runs deterministically: the execution time for each cycle of the code is the same. This makes the controller more stable when compared to regular operating systems such as Windows, where interrupts and other operations compromise the timing of the code. The system is equipped with a National Instruments BNC-2111 I/O card.

The desired force is set using a graphical user interface (GUI) by the practitioner and the damper modulates the resistance throughout the stroke (Fig. 7). After the stroke is complete the damper deactivates and the mechanical return system brings the handle back to its resting open position.

5 Graphical User Interface & Exercising

The software provides two GUIs to interact with the hand device: a) for the practitioner, b) for the patient.

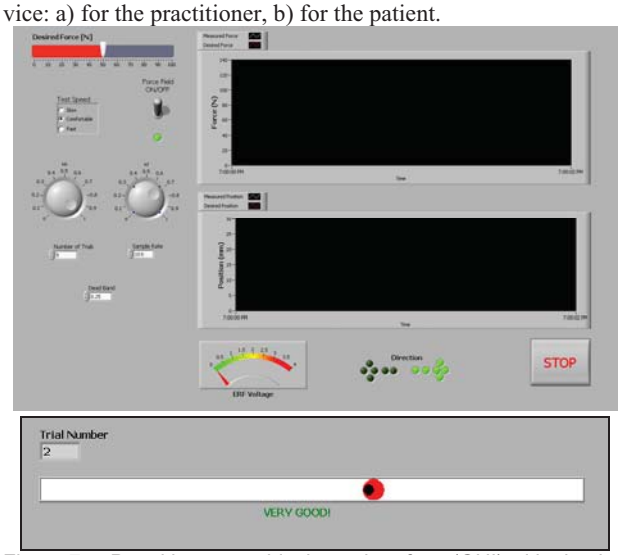

Figure 7. Practitioner graphical user interface (GUI) with simple game implemented at the VRHD installed at NU.

The practitioner GUI is shown in Fig. 8-TOP, which allows the practitioner to modify the parameters of the device. The desired force that the patient will feel during hand exercises may be adjusted by the slider at the top left side. The GUI also allows the practitioner to select the number of exercises and the speed of the exercise may be selected as fast, slow, or comfortable. Force and position are graphed and stored in a log file to provide better information to the practitioner regarding the patient's performance. Two knobs, at the left side, allow the practitioner to select the resistance felt during the "force field exercise".

Rehabilitation is often a long and painful process. To ease the process, and motivate the patient, a simple game interface has been implemented, referred here as the "force field exercise". The big red dot in Figure 7.BOTTOM moves with the speed configured by the practitioner. The patient tries to follow the red dot by squeezing the handle and the small black dot indicates the position of the handle. If the patient is squeezing faster than the motion of the red dot then a large force is being applied by

the damper that will delay the patient hand. If the patient hand is moving slower than the motion of the red dot, then the resistive force applied by the damper is reduced and this makes it easier for the patient to squeeze faster. If the black dot is within the red one then the damper and its controller are keeping the resistive force constant to that selected by the practitioner. In addition, the game makes comments according to the performance of the patient, thus motivating him/her. Fig. 8 shows the graphs from an exercise using the force field interface. As long as the position error is negative then the force is below the desired force Fd selected for this example to be equal to 50N. Once the error is around 0mm then the applied force is constant and equal to Fd. Finally, when the position error is positive, then the applied force is larger then Fd.

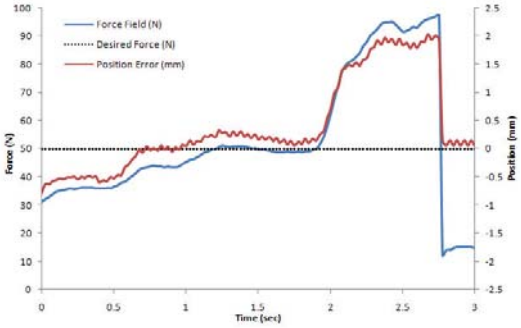

Figure 8. Position error and force applied during a force-field exercise using the VRHD.

6 MRI Compatibility Testing

A 3-Tesla Siemens Trio whole-body MRI equipped with 12-channel Siemens TIM head coil (Athinoula A. Martinos Center for Biomedical Imaging, Massachusetts General Hospital, Boston, MA) was utilized for all MRI compatibility tests conducted on the hand device. Images were collected using gradient-echo echo-planar imaging (GE-EPI), commonly used in functional imaging, as it is the sequence to be used with an operating the hand device. Acquisition parameters were: TR/TE=2000/30 ms, voxel size (3.1mm)×(3.1mm)×(5.0mm), 128×128 acquisition matrix/ 200mm×200mm FOV, 33 slices, 90^o flip angle. The imaging object was a plastic phantom designed to approximate the dimensions and proportions of the head and torso of a human subject [16]. The dimensions of the phantom are as follows: head portion: width, 16.5 cm; length, 28.3 cm; height, 15.25 cm; and torso portion: width, 43.2 cm; length, 59 cm; height, 15.25 cm. The phantom was filled with 45 liter of 1.24g $NiSO_4 \times 6\ H_2O$ / 2.62 NaCl per 1000g H_2O solution to simulate physiological T1 and T2 values of the MRI.

Figure 9. Experimental setup showing the Phantom and Hand Device during imaging

The power supply that supplied a high voltage to the hand device and the computer that reads the sensor data and controls the device were located outside of the MRI room. To minimize Electromagnetic Interface (EMI), the wires were properly shielded and cables of appropriate size and impedance were used. The cables were shielded by a braided copper meshing and passed through the penetration panel into the shielded MR room. The low amperage current required to activate the ERF ensures that the electromagnetic interference is kept to a minimum, both in the cables and the ERF components. The low amperage current also results in a low power consumption in the cables and ERF components which avoids increased temperature in the test device.

Tests were performed to demonstrate that the strong magnetic field of the scanner and sensitive functional imaging sequences doesn't affect the performance of the hand device in the MR environment. The performance of the linear potentiometer and force sensor was evaluated individually, and then the performance of the final hand device was examined. The individual components and the hand device were placed about 30-cm from the isocenter of the magnet, much closer than where the hand of the subject lying in the supine position will be located (Fig. 9).

The potentiometer was tested at two different conditions: a) the potentiometer measuring the static position (the shaft is not moving), b) the potentiometer measuring the dynamic position (the shaft is moving back and forth). In both cases, the data were low pass filtered. For the first condition, the potentiometer was tested in the zero and full length of the stroke while the output voltages were recorded in real time in the computer. For the second condition, the potentiometer was tested for the full range of displacement of the potentiometer shaft. Fig. 10 shows the voltage vs. time plot for the full displacement, during EPI scans.

The force sensor was tested during EPI scans at two different conditions: a) no force applied to the sensor that was sitting on the table, b) force applied to the sensor while it was being moved manually in the scanner. In both cases, the data were low pass filtered and for the second case are shown in Fig. 11.

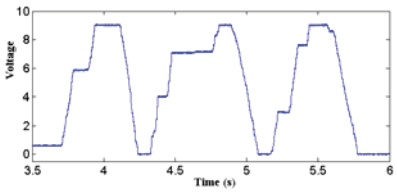

Figure 10. Output voltage versus time during full stroke motion

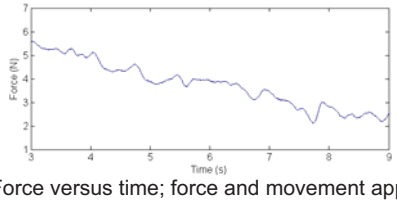

Figure 11. Force versus time; force and movement applied to the force sensor during EPI scans

Finally, the performance of the hand device in the MRI is shown in Fig. 12. A person is operating the device for the desired force of 100N, during EPI scans. As it is shown in the figures above, for both linear potentiometer and force sensor we can filter the data and use the sensors in the region of 30-cm distance from the isocenter of the magnet. The results show that the hand device performs without any problem in the MR environment.

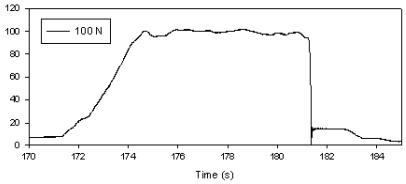

Figure 12. Performance of the hand device during EPI scans for desired force of 100N

Thorough testing was performed to study possible degrada-

tion of the MR images during the operation of the hand device during functional imaging. To ensure that using the hand device had no degradation in the MR images and to visualize the possible artifacts caused by the introduction of the device in the magnetic field, a series of phantom tests were conducted using the EPI sequence used for human imaging. The control image was acquired without any device in the MRI room (Fig. 13a). Then phantom EPI images were acquired in the presence of the hand device for the following conditions: i) all electronics were off (Fig. 13b), ii) all electronics were on but the device was not under operation (Fig. 13c), iii) the device was under operation by a person in the MRI room for the 100N desired resistive force (Fig. 13d). The phantom was not moved during the entire tests. As it is shown in Fig. 13, no image shift or distortion was observed in the image subtractions. Signal to noise ratio calculation was performed on the acquired images to ensure that the introduction and operation of the hand device caused no degradation in the MRI images. For more details on the SNR calculation, please see [15]. **Table 3** reports the SNR values obtained upon the operation of the hand device into the MRI scanner. In all cases, simple paired t-tests comparing the SNR of the condition to control image (two-tailed, P=0.05) failed to reach significance, with P-values ranging from 0.06 to 0.98.

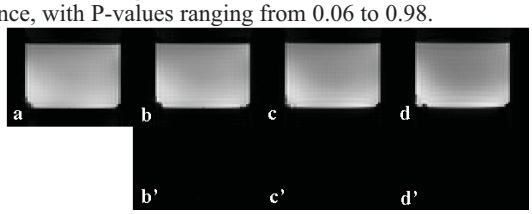

Figure 13. Effect of hand device on phantom images: (a-d), **(a)** control; **(b)** all electronics were off ; **(c)** MR all electronics were on but the device was not under operation; **(d)** the device was under operation by a person in the MRI room for the 100N desired resistive force; (b'-d') subtraction of the control (a) from (b-d).

Table 3, Signal Stability and SNR for Phantom Images Acquired with EPI

Condition	Signal (a.u.)	SNR [c]
Control (no device)	2086 ±204 [a]	189.63
Hand device in the scanner, all electronics were off	2065 ± 220 [b]	187.73
Hand device in the scanner, all electronics were on, the device was not under the operation	2044 ±198 [b]	185.81
Hand device in the scanner, all electronics were on, the device was under operation with 100N	2038 ± 212 [b]	185.27

[a] Values are, means of signal ROI ± standard deviation of the mean
[b] P-values ranging from 0.06 to 0.98 (two-tailed t-tests comparing condition to control; threshold set at P=0.05)
[c] SNR calculated dividing mean of signal ROI to width of the distribution of background intensities, $\sigma = 11$

7 Conclusions

A 1 DOF fMRI compatible force feedback device for hand grasp and release rehabilitation was presented. The device generates computer controlled resistive forces, measures the position (and through it calculates velocity and acceleration) and gripping force of the hand and enables isotonic, isokinetic, and isometric exercises. These properties were achieved by utilizing ERFs, which can produce large resistive forces upon activation with an electric field; an optical encoder; and a force sensor. We evaluated the grip strength of individual post stroke performing repetitive grasp and release movements to define the acceptance range of resistive forces applied by VRHD to the hand. A GUI for the practitioner and the patient were developed to facilitate interaction with the device. A series of MRI compatibility experiments demonstrate that the scanning environment didn't interfere with the ability to generate controllable resistive forces with ER fluid damper, and accurately record handle motion and handgrip strength with utilizing the position and force sensors. Current work includes pre-clinical testing of the device with stroke patients and human subject testing of the device in the MRI environment.

Acknowledgments

This work was supported by WGI Inc., Southwick, MA, USA. The help provided by Marlena Pelliccio, Fernanda Romaguera, and Chiara Mancinelli in the physical therapy evaluations is acknowledged and appreciated.

References

[1] "Heart Disease and Stroke Statistics—2005 Update.," American Heart Association, Dallas, Texas 2005.
[2] P. S. Lum, C. G. Burgar, P. C. Shor, M. Majmundar, and M. Van der Loos, "Robot-assisted movement training compared with conventional therapy techniques for the rehabilitation of upper-limb motor function after stroke," *Arch Phys Med Rehabil,* vol. 83, pp. 952-9, Jul 2002.
[3] H. I. Krebs, B. T. Volpe, M. Ferraro, S. Fasoli, J. Palazzolo, B. Rohrer, L. Edelstein, and N. Hogan, "Robot-aided neurorehabilitation: from evidence-based to science-based rehabilitation," *Top Stroke Rehabil,* vol. 8, pp. 54-70, Winter 2002.
[4] D. Jack, R. Boian, A. S. Merians, M. Tremaine, G. C. Burdea, S. V. Adamovich, M. Recce, and H. Poizner, "Virtual reality-enhanced stroke rehabilitation," *IEEE Trans Neural Syst Rehabil Eng,* vol. 9, pp. 308-18, Sep 2001.
[5] J. B. Rowe and R. S. Frackowiak, "The impact of brain imaging technology on our understanding of motor function and dysfunction," *Curr Opin Neurobiol,* vol. 9, pp. 728-34, Dec 1999.
[6] J. Diedrichsen, Y. Hashambhoy, T. Rane, and R. Shadmehr, "Neural correlates of reach errors," *J Neurosci,* vol. 25, pp. 9919-31, Oct 26 2005.
[7] R. Gassert, R. Moser, E. Burdet, and H. Bleuler, "MRI/fMRI-compatible robotic system with force feedback for interaction with human motion," *IEEE/ASME Transactions on Mechatronics,* vol. 11, pp. 216 - 224 2006.
[8] J. Hidler, T. Hodics, B. Xu, B. Dobkin, and L. G. Cohen, "MR compatible force sensing system for real-time monitoring of wrist moments during fMRI testing," *J Neurosci Methods,* vol. 155, pp. 300-307, Sep 15 2006.
[9] J. D. Schaechter, C. Stokes, B. D. Connell, K. Perdue, and G. Bonmassar, "Finger motion sensors for fMRI motor studies," *Neuroimage,* vol. 31, pp. 1549-59, Jul 15 2006.
[10] S. J. Graham, W. R. Staines, A. Nelson, D. B. Plewes, and W. E. McIlroy, "New devices to deliver somatosensory stimuli during functional MRI," *Magn Reson Med,* vol. 46, pp. 436-42, 2001.
[11] G. S. Harrington, C. T. Wright, and J. H. Downs, 3rd, "A new vibrotactile stimulator for functional MRI," *Hum Brain Mapp,* vol. 10, pp. 140-5, Jul 2000.
[12] A. C. Zappe, T. Maucher, K. Meier, and C. Scheiber, "Evaluation of a pneumatically driven tactile stimulator device for vision substitution during fMRI studies," *Magn Reson Med,* vol. 51, pp. 828-34, Apr 2004.
[13] A. Khanicheh, A. Muto, C. Triantafyllou, B. Weinberg, L. Astrakas, A. Tzika, and C. Mavroidis, "fMRI-compatible rehabilitation hand device," *J Neuroeng Rehabil,* vol. 3, p. 24, 2006.
[14] A. Khanicheh, D. Mintzopoulos, B. Weinberg, A. A. Tzika, and C. Mavroidis, "MR_CHIROD v.2: magnetic resonance compatible smart hand rehabilitation device for brain imaging," *IEEE Trans Neural Syst Rehabil Eng,* vol. 16, pp. 91-8, Feb 2008.
[15] A. Khanicheh, D. Mintzopoulos, B. Weinberg, A. A. Tzika, C. Mavroidis, "Evaluation of electrorheological fluid dampers for applications at 3-Tesla MRI environment," *IEEE / ASME Transactions on Mechatronics*, Vol. 13, No. 3, pp. 286-294, 2008.
[16] F. G. Shellock, D. S. Fieno, L. J. Thomson, T. M. Talavage, D. S. Berman, "Cardiac pacemaker: In vitro assessment at 1.5 T," *American Heart Journal*, vol. 151, pp 436-443.